(NASA-CR-134788) CHARACTERISTICS OF RESPONSE FACTORS OF COAXIAL GASEOUS ROCKET INJECTORS (Georgia Inst. of Tech.) 43 p HC $3.75 CSCL 21H

N75-20466

Unclas
G3/20 14690

NASA CR-134788

CHARACTERISTICS OF RESPONSE FACTORS OF COAXIAL GASEOUS ROCKET INJECTORS

by

B. A. Janardan
B. R. Daniel
B. T. Zinn

GEORGIA INSTITUTE OF TECHNOLOGY
ATLANTA, GEORGIA 30332

prepared for

NATIONAL AERONAUTICS AND SPACE ADMINISTRATION

NASA Lewis Research Center
Grant NGL 11-002-085
Richard J. Priem, Project Manager

Requests for copies of this report should be referred to:

National Aeronautics and Space Administration
Scientific and Technical Information Facility
P.O. Box 33
College Park, Md. 20740

1. Report No.	2. Government Accession No.	3. Recipient's Catalog No.
NASA CR-134788		

4. Title and Subtitle	5. Report Date
CHARACTERISTICS OF RESPONSE FACTORS OF COAXIAL GASEOUS ROCKET INJECTORS	March 1975
	6. Performing Organization Code
7. Author(s)	8. Performing Organization Report No.
B. A. Janardan, B. R. Daniel and B. T. Zinn	
	10. Work Unit No.
9. Performing Organization Name and Address	11. Contract or Grant No.
Georgia Institute of Technology Atlanta, Georgia 30332	NGL 11-002-085
	13. Type of Report and Period Covered
12. Sponsoring Agency Name and Address	Contractor Report
National Aeronautics and Space Administration Washington, D. C. 20546	14. Sponsoring Agency Code

15. Supplementary Notes

Technical Monitor, Richard J. Priem, NASA Lewis Research Center, 21000 Brookpark Road, Cleveland, Ohio 44135

16. Abstract

In this report the results of an experimental investigation undertaken to determine the frequency dependence of the response factors of various gaseous propellant rocket injectors subject to axial instabilities are presented. The injector response factors were determined, using the modified impedance-tube technique, under cold-flow conditions simulating those observed in unstable rocket motors. The tested injectors included a gaseous-fuel injector element, a gaseous-oxidizer injector element and a coaxial injector with both fuel and oxidizer elements. Emphasis was given to the determination of the dependence of the injector response factor upon the open-area ratio of the injector, the length of the injector orifice, and the pressure drop across the injector orifices. The measured data are shown to be in reasonable agreement with the corresponding injector response factor data predicted by the Feiler and Heidmann model.

17. Key Words (Suggested by Author(s))	18. Distribution Statement
Combustion instability Gaseous rocket Injector Response factor	Unclassified - unlimited

19. Security Classif. (of this report)	20. Security Classif. (of this page)	21. No. of Pages	22. Price*
Unclassified	Unclassified	36	$3.00

* For sale by the National Technical Information Service, Springfield, Virginia 22151

SUMMARY

In this report the results of an experimental investigation undertaken to determine the frequency dependence of the response factors of various gaseous propellant rocket injectors subject to axial instabilities are presented. The injector response factors were determined, using the modified impedance-tube technique, under cold-flow conditions simulating those observed in unstable rocket motors. The tested injectors included a gaseous-fuel injector element, a gaseous-oxidizer injector element and a coaxial injector with both fuel and oxidizer elements. Emphasis was given to the determination of the dependence of the injector response factor upon the open-area ratio of the injector, the length of the injector orifice, and the pressure drop across the injector orifices. The measured data are shown to be in reasonable agreement with the corresponding injector response factor data predicted by the Feiler and Heidmann model.

TABLE OF CONTENTS

PRECEDING PAGE BLANK NOT FILMED

LIST OF ILLUSTRATIONS

INTRODUCTION

The stability of the combustor of a rocket motor depends upon the wave-energy balance between the various gain and loss mechanisms that are present in the system. The primary source of wave-energy gain is the combustion process. Wave-energy losses are provided by the mean flow, the nozzle, and mechanical damping devices (e.g., acoustic liners) which may be present in the system. As the stability of a rocket motor depends upon the difference between the gain and loss mechanisms, it is of utmost importance that quantitative data capable of describing the damping provided by the loss mechanisms and the driving provided by the unsteady combustion process must be available. Furthermore, an understanding of the dependence of these gain and loss mechanisms upon engine design parameters and operating conditions is needed. The investigation described in this report was undertaken for the purpose of obtaining a better understanding of the driving provided by the unsteady combustion process; specifically, this investigation was concerned with the acquisition of experimental data that quantitatively describes the manner in which various injector designs affect the energy gain provided by the unsteady combustion process.

The injector elements of a gaseous rocket motor control the steady state gas flow and heat transfer patterns inside the combustion chamber. In addition, the injector design influences the response of the flow rate through the injector to combustion chamber disturbances. The characteristics of this response have a profound effect upon engine stability. Customarily, the influence of the injector upon the chamber stability is described by an injector response factor which describes the manner in which the propellants' burning rate responds to a given pressure oscillation in the chamber. The injector response factor basically accounts for the dependence of the unsteady burning rate upon both the unsteady combustion process and unsteady flow of propellants through the injector elements. This response factor can be used to evaluate the energy added by the combustion process into the disturbance in the combustion chamber. It can also be used as the injector end boundary condition that needs to be satisfied in a stability analysis of a gaseous rocket combustion chamber.

Most of the available experimental investigations[1-7] on the behavior of gaseous propellant injectors were concerned with the steady operation of these devices with little or no consideration being given to the corresponding unsteady problem. In contrast, the analytical studies of Feiler and Heidmann were concerned with the predictions of the characteristics of the response factor of a gaseous injector element. In the Feiler and Heidmann analysis,[8,9] a single gaseous hydrogen injector element is modeled as a combination of lumped flow elements. The desired expressions for the injector response factor are then obtained by solving the conservation equations that describe the unsteady flow inside the various components of the injector. The resulting expressions describe the dependence of the injector response factor upon the injector geometry and the flow conditions in the chamber and the injector. In this analytical model, combustion is assumed to be concentrated in front of the injector face and the effects of mixing and chemical reactions are accounted for by the introduction of an as yet unknown time delay τ_b^*. The period τ_b^* describes the time required for the gaseous oxidizer and fuel streams to mix and burn. In Ref. 10, the Feiler and Heidmann predictions[8] have been modified to account for the compressibility of the gaseous streams flowing through the injector elements.

The results of Refs. 8 and 10 indicate that for a given frequency range and for certain ranges of the parameter τ_b^*, various injector designs can indeed result in the amplification of chamber disturbances. When τ_b^* is identically zero, which corresponds to the case of no combustion present in the system, the results of Refs. 8 and 10 indicate that under these conditions the injector acts as a mechanical damping device; a situation that is to be expected from related studies of Helmholtz resonators and acoustic liners.

Although the predictions of the Feiler and Heidmann analysis have been known for a number of years, they have never been verified experimentally. It is one of the objectives of this investigation to provide experimental data that could be used to check the validity of the Feiler and Heidmann model. In addition, this investigation is concerned with providing experimental data that will quantitatively describe the manner in which various coaxial injector designs affect the stability of gaseous propellant rocket motors. In pursuit of the above-mentioned objectives, the response factors of a number of gaseous rocket injector configurations have been measured under cold-flow conditions simulating those observed in rocket motors experiencing axial instabilities. Specifically, the response factor of configurations that simulate the flow conditions in a gaseous-fuel injector element, a gaseous-oxidizer injector element, and a coaxial injector with both fuel and oxidizer elements have been determined using the modified impedance-tube technique. The measured injector response factor data are presented and the results discussed in this report.

NOMENCLATURE

A	area
C	Capacitance, defined by Eq. (4)
c	speed of sound
I	Inductance, defined by Eq. (4)
L	length of the injector orifice
l_{eff}	effective orifice length given by Eq. (14)
M	Mach number
N	nondimensional injector response factor
P	pressure
R	Resistance, defined by Eq. (4)
V	injector dome volume
W	mass flow rate of propellant
Y	admittance
y	nondimensional admittance
α	admittance parameter defined by Eq. (7)
β	admittance parameter defined by Eq. (8)

γ	specific heat ratio
δ	equal to $(\bar{P}_d^* - \bar{P}_c^*)/\bar{P}_c^*$
λ	wavelength
ρ	density
σ	open-area ratio of the injector
τ	time lag
ω	angular frequency

Superscripts

$(\bar{\ })$	steady state quantity
$(\ )^*$	dimensional quantity
$(\ )'$	perturbation quantity

Subscripts

$(\ )_b$	associated with the combustion process
$(\ )_c$	evaluated in the chamber
$(\ )_d$	evaluated in the injector dome
$(\ )_f$	associated with the fuel
$(\ )_{ox}$	associated with the oxidizer
$(\ )_s$	evaluated at the injector surface
$(\ )_1$	evaluated at injector orifice entrance
$(\ )_2$	evaluated at injector orifice exit

ANALYTICAL CONSIDERATIONS

The ability to quantitatively describe the injector response factor is of great practical importance since the combined response of the injector flow rate and the combustion process to chamber disturbances is the mechanism responsible for amplifying and maintaining combustion instability oscillations. In an effort to develop an analytical technique for the prediction of the response factor of a gaseous injector, Feiler and Heidmann [8, 9] analyzed in detail the unsteady flow through the gaseous hydrogen injector element shown in Fig. 1. Combustion is assumed to occur a certain distance downstream of the injector exit plane and the response of the injector flow rate to a small amplitude pressure oscillation in the chamber is determined by analyzing the linearized conservation equations for each of the injector components. Assuming that each of the injector components behaves as a lumped element, and applying the Laplace transform to the linearized conservation equations, the relationships presented in Fig. 1 are obtained. By appropriate manipulations of these equations and setting the Laplace operator s equal to iω, which implies a sinusoidal time dependence of the perturbations, the following expression for the injector response factor was obtained:

$$N = \frac{W_b'}{P_c'} = \left(\frac{W'_{b_{max}}}{P'_{c_{max}}}\right) e^{i\theta} \tag{1}$$

where

$$\frac{W'_{b_{max}}}{P'_{c_{max}}} = \frac{-1}{R_2\left\{\left[\frac{R_1}{C^*\omega^*} - I^*\omega^*\right]^2 + \left[2\left(\frac{R_1 \Delta P_1^*}{\bar{P}_d^*} + \frac{\Delta P_2^*}{\bar{P}_2^*}\right)\right]^2\right\}^{\frac{1}{2}}} \tag{2}$$

$$\theta = \frac{\pi}{2} - \omega^* \tau_b^* - \arctan \frac{2\left\{\frac{R_1 \Delta P_1^*}{\bar{P}_d^*} + \frac{\Delta P_2^*}{\bar{P}_2^*}\right\}}{\left\{\frac{R_1}{C^*\omega^*} - I^*\omega^*\right\}} \tag{3}$$

and

$$C^*\omega^* = \left(\bar{\rho}_d^* V^*/\gamma \bar{W}^*\right)\omega^* \quad ; \quad I^*\omega^* = \left[\bar{W}^*\left(L^*/A_1^*\right)/g\bar{P}_2^*\right]\omega^* \tag{4a}$$

$$\frac{\Delta P_1^*}{\bar{P}_d^*} = \left(\bar{P}_d^* - \bar{P}_1^*\right)/\bar{P}_d^* \quad ; \quad \frac{\Delta P_2^*}{\bar{P}_2^*} = \left(\bar{P}_2^* - \bar{P}_c^*\right)/\bar{P}_2^* \tag{4b}$$

$$R_1 = \frac{\bar{P}_d^*}{\bar{P}_1^* - \left(\Delta P_1^*/\gamma\right)} \; ; \quad R_2 = \frac{\bar{P}_2^*}{\bar{P}_c^* - \left(\Delta P_2^*/\gamma\right)} \tag{4c}$$

The quantity τ_b^* appearing in Eq. (3) is the residence time of a propellant mass element in the combustor prior to its combustion; τ_b^* is identically zero when there is no combustion in the system. The parameters appearing in Eq. (4) depend upon the injector geometry and engine operating conditions, and their influence upon the injector element response factor is also of interest to rocket designers.

Expressions similar to those developed above for the gaseous-fuel injector element can also be developed for the gaseous-oxidizer injector element. The total response, N_t, of a coaxial gaseous injector element can then be obtained, by substituting the expressions for the fuel and oxidizer response factors into the following equation:

$$N_t = \frac{W_t'}{P'} = \frac{\left(W_t^*\right)'/\bar{W}_t^*}{(P^*)'/\bar{P}^*} = \frac{\left\{\left(W_{ox}^*\right)' + \left(W_f^*\right)'\right\}/\bar{W}_t^*}{(P^*)'/\bar{P}^*} \tag{5}$$

$$= \left[\frac{\bar{W}_{ox}^*}{\bar{W}_t^*}\right] N_{ox} + \left[\frac{\bar{W}_f^*}{\bar{W}_t^*}\right] N_f \tag{5}$$

where N_{ox} and N_f respectively represent the response factors of the oxidizer and fuel injector elements while $\bar{W}_{ox}^*/\bar{W}_t^*$ and $\bar{W}_f^*/\bar{W}_t^*$ represent the ratios of the mean oxidizer and fuel flow and the total mean flow, respectively.

RESPONSE FACTOR DETERMINATION

The required injector response factor data were determined in this investigation from injector admittance data measured by use of the modified impedance-tube technique. The impedance tube setup shown in Fig. 2, consists of a 6-inch diameter cylindrical tube with a sound source capable of generating harmonic waves of desired frequency placed at one end. The injector element under investigation is placed at the other end. During an experiment, the flow of a gaseous propellant through the injector is simulated by the flow of air. Regulating valves are provided to ensure that the pressure drop across the injector orifices is maintained at a required value. By means of an acoustic driver, a standing wave pattern of a given frequency is excited in the tube and a microphone probe is traversed along the tube to measure the axial variation of the standing pressure wave pattern. As explained in the next section, the admittance of the injector end of the impedance-tube is determined from the measured axial variation of the standing pressure wave. The frequency dependence of the admittance and the response factor of the injector is determined by repeating the experiment at different frequencies.

The first step in the determination of the injector response factor N consists of the measurement of the "average" surface admittance Y_s^* at the injector end of the modified impedance tube. The "average" surface admittance is defined as the ratio of the "average" normal velocity perturbation across the injector surface and the local pressure perturbation; that is:

$$Y_s^* = \frac{\underset{\rightarrow}{u}_s^{*\prime} \cdot \underset{\rightarrow}{n}}{p_s^{*\prime}} \qquad (6)$$

The admittance Y_s^* is a complex number whose real and imaginary parts describe the relationships that exist at the location under consideration between the amplitudes and phases of the velocity and pressure perturbations.

From a physical point of view it is more satisfying to describe the admittance by means of two parameters α and β which respectively describe changes in amplitudes and phases between the incident and reflected pressure waves at the location under consideration; that is:

$$\left[\frac{\text{Amplitude of Reflected Pressure Wave}}{\text{Amplitude of Incident Pressure Wave}}\right]_{\substack{\text{Injector}\\ \text{Face}}} = e^{-2\pi\alpha} \tag{7}$$

$$\left[\begin{matrix}\text{Phase change Between Incident and}\\ \text{Reflected Pressure Waves}\end{matrix}\right]_{\substack{\text{Injector}\\ \text{Face}}} = \pi(1 + 2\beta) \tag{8}$$

The parameter β appearing above satisfies the condition $|\beta| \leq 0.5$.

The expressions required for the calculation of the injector surface admittance are obtained from solutions of the system of conservation equations which describe the behavior of small amplitude, one-dimensional waves inside an impedance-tube containing a steady one-dimensional flow. These solutions are required to satisfy an admittance boundary condition at the injector surface in terms of the as yet unknown parameters α and β. The resulting expressions (See Ref. 12 for detailed derivations of these solutions), describing the time and space dependence of the pressure and velocity perturbations at the injector surface, are substituted into Eq. (6) to obtain an expression for the injector surface admittance. Normalizing the resulting expression with the characteristic admittance $Y_g^* = 1/\bar{\rho}^*\bar{c}^*$ of the gas medium, the following expression for the nondimensional injector surface admittance y_s is obtained[12]:

$$y_s = \frac{Y_s^*}{Y_g^*} = \Gamma + i\eta = \coth \pi(\alpha - i\beta) \tag{9}$$

It can also be shown[12] that the parameters α and β, which appear in Eqs. (7), (8) and (9) must satisfy the following relationships between variables describing the characteristics of the standing wave pattern:

$$\alpha = \frac{1}{\pi}\tanh^{-1}\left[\frac{|P^*_{min}|}{|P^*_{max}|}\right]; \quad \beta = \frac{2Z^*_{min}}{\lambda^*} \tag{10}$$

In impedance-tube experiments and in the present study, the relationships presented in Eq. (10) are used to determine the admittance variables α and β. The procedure leading to the determination of α and β consists of measuring (a) the distance Z^*_{min} from the injector surface to the first pressure amplitude minimum and (b) the ratio of $|P^*_{min}|/|P^*_{max}|$ of the minimum pressure amplitude to the maximum pressure amplitude. The resulting values of α and β are then substituted into Eq. (9) to obtain the injector surface admittance.

From the measured injector surface admittance y_s, the injector orifice admittance y_2 is determined by using the following relationship obtained from the perturbed form of mass conservation law:

$$(u^*)_s' A_s^* = (u^*)_2' A_2^*$$

which upon dividing by $(P^*)_s'$ gives

$$y_2 = y_s/\sigma \tag{11}$$

where $\sigma = A_2^*/A_s^*$ is the injector open-area ratio. In deriving Eq. (11) the gas has been assumed to be incompressible; an allowable assumption for the situation under consideration.

An expression relating the nondimensional response factor N to the nondimensional admittance y is obtained from the definitions of these two quantities as follows:

$$N = \frac{\vec{W}^{*\prime} \cdot \vec{n}/\bar{W}^{*}}{p^{*\prime}/\bar{p}^{*}} = \frac{\bar{p}^{*}}{\bar{\rho}^{*}\bar{u}^{*}}\left[\bar{\rho}^{*}\,\frac{\vec{u}^{*\prime} \cdot \vec{n}}{p^{*\prime}} + \frac{\rho^{*\prime}}{p^{*\prime}}\,\vec{\bar{u}}^{*} \cdot \vec{n}\right]$$

$$= \frac{1}{\gamma\bar{M}}\left[\bar{\rho}^{*}\bar{c}^{*}\;\frac{\vec{u}^{*\prime} \cdot \vec{n}}{p^{*\prime}} + \vec{\bar{M}} \cdot \vec{n}\right]$$

$$= \frac{1}{\gamma\bar{M}}\left(y + \vec{\bar{M}} \cdot \vec{n}\right) \tag{12}$$

In deriving Eq. (12) it has been assumed that the gas is perfect and that the oscillations are isentropic. The response factor N of the test injectors is finally obtained by substituting the measured orifice admittance y_2 into Eq. (12) which can be rewritten in the following form for the experimental setup of this investigation:

$$N = \frac{1}{\gamma}\left[-\frac{y_2}{\bar{M}_2} + 1\right] \tag{13}$$

TEST INJECTORS

In order to obtain the needed data, the frequency dependence of the response factors of the injector configurations shown in Figs. 3 through 6 have been determined. The characteristic dimensions of these injectors, namely, the injector orifice open-area ratio, the orifice length, and the injector dome volume are also presented in the above-mentioned figures.

Injector configurations 1 and 2 were designed to simulate the flow behavior through gaseous-fuel injector elements. The dimensions of these configurations were chosen to provide data capable of determining the effect of the injector open-area ratio upon the injector response factor. Injector configurations 3 through 5 were designed to simulate the flow behavior in gaseous-oxidizer injector elements, and their dimensions were chosen to allow the determination of the dependence of the injector response factor upon the orifice length. Injector configuration 6, shown in Fig. 6, consists of a combination of configurations 1 and 3. This configuration was designed to simulate the flow behavior in a coaxial injector of a gaseous rocket motor. This injector configuration was tested to check the validity of Eq. (5) by comparing its measured response factors with predicted response factor data obtained by substituting the individually-predicted response factors of configurations 1 and 3 into Eq. (5).

RESULTS

Introduction

The results presented in this section were obtained by measuring the admittances and response factors of the test injectors over the frequency range of 150 to 800 Hz which included their resonant frequency. To establish the repeatability of the experimental data, the frequency dependence of the response factor one of the test injectors was measured on two different occasions and the response factor data obtained in these tests are presented in Fig. 7. An examination of this figure indicates that the measurement technique yields repeatable data. The scatter observed in the measured values of the imaginary part of the response factor is due to the fact that at the corresponding frequencies the standing wave in the impedance tube had a flat minima and hence its axial location could not be precisely measured.

Before presenting the results, it is necessary to point out a difference between the geometrical configurations of the injector elements whose admittances were measured in this study and the injector configurations considered in the theoretical model of Feiler and Heidmann.[8] The theoretical analysis considers the behavior of a single injector element and its predictions provide a response factor that is valid at the exit plane of the injector orifice. As it would be extremely difficult to directly measure the response factor of a single injector element, this study undertook the measurement of the response factors of configurations containing either 5 or 13 injector elements. As stated earlier, the admittances measured in this study represent "average" admittances over the tested injector surface. Hence, before any meaningful comparisons between the predicted and the measured sets of admittance data can be made, the above-mentioned difference must be suitably taken into consideration. This point was discussed in the previous section where it was shown that by using mass conservation considerations, this difference can be accounted for by multiplying the theoretically predicted orifice admittances by the open-area ratio σ of the injector configuration. This step "averages" the predicted orifice admittance over the injector surface. To illustrate this point, the theoretically predicted frequency dependence of the admittances of injector configuration 1 with a pressure drop δ of 0.068 across the injector orifices is presented in Fig. 8. The broken lines in this figure describe the admittances at the exit plane of the injector orifices while the solid lines represent the "average" admittances of the injector surface. It is this "average" data which has to be compared with the admittances measured during this investigation.

In the present study, the expressions provided by Feiler and Heidmann[8] have been slightly modified when used to compute the predicted admittances and response factors of the test injector configurations. This was necessitated by the observation that the measured resonant frequencies of the tested injectors did not coincide with their predicted values. This is illustrated by the data presented in Fig. 9. The broken line in this figure describes the theoretically predicted frequency dependence of the real and imaginary parts of the response factor of one of the test injectors. An examination of this figure indicates that while the two sets of data are similar in magnitude and shape, the observed injector resonant frequency is lower than its predicted value. In an effort to explain this frequency shift, use was made of knowledge developed in studies concerned with the behavior of Helmholtz resonators and acoustic liners[13, 14] where it has been well known that the effective length of the slug of the gaseous mass oscillating within the orifice is longer than the orifice length.

It is also well known that the resonant frequencies of Helmholtz resonators and acoustic liners are inversely proportional to the square root of the orifice length. This suggests that the actual length L^* of the injector orifices should be replaced by an effective length l^*_{eff} whenever it appears in the analytical expressions of the Feiler and Heidmann analysis. From experimental reactance data of acoustic liners with apertures of various thicknesses, Garrison[13] developed the following empirical relation for the effective length l^*_{eff}:

$$l^*_{eff} = L^* + 0.85\left[1 - 0.70\sqrt{\sigma}\right]\left(D^*_o - D^*_i\right) \tag{14}$$

where D^*_o and D^*_i are respectively the outer and inner diameters of the orifices. Computing the predicted response factor data of the test injector with L^* replaced by the effective length l^*_{eff}, the result indicated by the solid line in Fig. 9 was obtained. The experimental resonant frequency now is in better agreement with the predicted resonant frequency than the original Feiler and Heidmann prediction. Based on this result all of the theoretically predicted data presented in the remainder of this report was obtained by suitably incorporating Eq. (14) into the expressions of Ref. 8.

Comparison of Measured and Predicted Injector Admittances

The injector admittances measured during the course of the present study are presented in Figs. 10 through 14 along with admittance data predicted by the Feiler and Heidmann model. These figures describe, respectively, the frequency dependence of the real and imaginary parts of the surface admittances of injector configurations 1 through 5. An examination of these figures indicates a reasonable agreement between the measured and predicted admittances. The discrepancy observed in the data may be, among other factors, due to the fact that radial pressure gradients were measured in the domes of some of the tested injectors. These pressure gradients resulted in different pressure drops across different injector elements. The possibility of such pressure gradients is not considered in the theoretical model[8] and their effect cannot be accounted for in predicting the injectors' response factors. The theoretical admittances obtained in this study were computed assuming that the pressure drops across all of the injector orifices were equal to the pressure drop measured across one of the outer injector elements; an assumption that is contrary to the above-mentioned observations.

The response factors of injector configurations 1 through 5 were obtained by substituting the measured admittance data into Eq. (13). As suggested in Ref. 8, the response factor data for the injectors tested in this program, with different pressure drops, are plotted in Fig. 15 in terms of a generalized response factor φ defined as

$$\varphi = N_{Real} \left\{ 2R_2 \left(\frac{R_1 \Delta P_1^*}{\bar{P}_d^*} + \frac{\Delta P_2^*}{\bar{P}_2^*} \right) \right\} \tag{15}$$

and a generalized reactance Ψ defined as

$$\Psi = \left(\frac{R_1}{C^* \omega^*} - I^* \omega^* \right) / 2 \left(\frac{R_1 \Delta P_1^*}{\bar{P}_2^*} + \frac{\Delta P_2^*}{\bar{P}_2^*} \right) \tag{16}$$

An examination of Fig. 15 indicates a reasonable agreement between the experimental data and the predictions of the Feiler and Heidmann model. Furthermore, this plot points to a convenient way for correlating and plotting injector response factor data.

Effect of Injector Design Parameters Upon Injector Response Factors

During this investigation, the dependence of the injector response factors upon the pressure drop across the injector orifices, the open-area ratio of the injector and the length of the injector orifices were investigated. The dependence of the injector response upon the pressure drop across the injector orifices is demonstrated by the data presented earlier in Figs. 10 through 14. An examination of these figures indicates that the injector admittances and response factors decrease rapidly in magnitude with increase in pressure drop across the orifices. Increase in pressure drop results in an increase in the resistance of the injector plate. This decreases the coupling between the pressure oscillation inside the injector dome and the pressure oscillation in the combustor in front of the injector plate. The increase in the injector pressure drop is observed, however, to have little effect upon the resonant frequency of the injector.

In order to determine the dependence of the injector response factor upon the injector characteristic dimensions, the admittance data measured with test configurations 1, 4 and 5 were substituted into Eq. (13) and the response factors obtained are presented in Figs. 16 and 17. The data presented in Fig. 16 describes the effect of the open-area ratio upon the injector response factor for a given orifice length and mass flux through the injector orifices. An examination of Fig. 16 indicates that an increase in the open-area ratio of the injector results in an increase in the damping provided by the injector. In addition, the data indicates an increase in the resonant frequency which is to be expected from results of studies on Helmholtz resonantors. The increase in the injector damping is due to the fact that for a given mass flux an increase in the open-area ratio results in a decrease in the pressure drop across the orifices. This in turn decreases the injector resistance. From a stability point of view this seems to suggest that, for a given mass flow across the injector plate, an injector should be designed with as large an open-area ratio as possible. However, in contemplating such changes in actual systems, one should also consider how an increase in the open-area ratio would affect other gain or loss mechanism in the system. For example, in an actual gaseous propellant rocket motor a decrease in the pressure drop across the injector orifices also affects the mixing rate and hence the propellants burning rate.

For a given open-area ratio and pressure drop across the orifices, data describing the effect of the orifice length upon the injector response factor is presented in Fig. 17. An examination of this figure indicates that an increase in the orifice length from 0.875" to 1.75" resulted in a decrease in the resonant frequency of the injector. Further examination of Fig. 17 indicates that although there is no observable change in the magnitude of the response factor at resonance, an increase in the orifice length decreases the band width of the response curve.

CONCLUSIONS

The measured data indicates that under the test conditions encountered in this study, there is reasonable agreement between the measured injector response factors and those predicted by the Feiler and Heidmann model. The good agreement observed between the measured and predicted total response factors of coaxial injectors containing both fuel and oxidizer elements suggests that the procedure suggested by Feiler and Heidmann for calculating the total response factors from individual injector response factor data is indeed valid.

The measured response factor data indicates that the orifice length can be varied to shift the resonant frequency of the injector without any change in the magnitude of the response factor at resonance. However, changes in pressure drop across the orifices and the open-area ratio of the injector were found to have a considerable effect on the injector response factor.

The injector configurations investigated in this program were similar to Helmholtz Resonators with a steady through flow. The interaction of such a configuration with a sound wave is not expected to produce any wave amplification, as was recognized by Feiler and Heidmann and confirmed by the data reported in this report. When a time delay, τ_b^*, due to combustion is added to the theoretical model, the phase relationship between the pressure and velocity perturbations required for wave amplification (and instability) is obtained. To test the latter hypothesis, and in the process measure the characteristic combustion time, τ_b^*, additional studies that will measure the response factors of "reacting" gaseous rocket injectors, under a variety of conditions simulating those observed in unstable engines, are needed.

REFERENCES

1. Falkenstein, G. L. and Domokos, S. J., "High Pressure Gaseous Hydrogen/Gaseous Oxygen Thrusters," AIAA/SAE 7th Propulsion Conference, Salt Lake City, Utah, AIAA Paper No. 71-737, June 1971.
2. Gregory, J. W. and Herr, P. N., "Hydrogen-Oxygen Space Shuttle ACPS Thruster Technology Review," AIAA/SAE 8th Propulsion Conference, New Orleans, Louisiana, AIAA Paper No. 72-1158, November 1972.
3. Paster, R. D., Lauffer, J. R., and Domokos, S. J., "Low Pressure Gaseous Hydrogen/Gaseous Oxygen Auxiliary Rocket Engines," AIAA/SAE 7th Propulsion Conference, Salt Lake City, Utah, AIAA Paper No. 71-738, June 1971.
4. Nagai, C. K., Gurnitz, R. N., and Clapp, S. D., "Cold-Flow Optimization of Gaseous Oxygen/Gaseous Hydrogen Injectors for the Space Shuttle APS Thrustor," AIAA/SAE 7th Propulsion Conference, Salt Lake City, Utah, AIAA Paper No. 71-673, June 1971.
5. Kors, D. L. and Calhoon, D. F., "Gaseous Oxygen/Gaseous Hydrogen Injector Element Modeling," AIAA/SAE 7th Propulsion Conference, Salt Lake City, Utah, AIAA Paper No. 71-674, June 1971.
6. Calhoon, D. F., Ito, J. I., and Kors, D. L., "Investigation of Gaseous Propellant Combustion and Associated Injector/Chamber Design Guidelines," NASA CR-121234, July 1973.
7. Burick, R. J., "Optimum Design of Space Storable Gas/Liquid Coaxial Injectors," Journal of Spacecraft and Rockets, Vol. 10, No. 10, pp. 663-670, October 1973.
8. Feiler, C. E. and Heidmann, M. F., "Dynamic Response of Gaseous Hydrogen Flow System and its Application to High Frequency Combustion Instability," NASA TN D-4040, June 1967.
9. Harrje, D. T., Editor, Liquid Propellant Rocket Combustion Instability, NASA SP-194, 1972.
10. Priem, R. J. and Yang, J. Y. S., "Technique for Predicting High Frequency Stability Characteristics of Gaseous Propellant Combustors," NASA TN D-7406, October 1973.
11. Morse, P. M. and Ingard, K. V., Theoretical Acoustics, McGraw Hill,

New York, 1968.

12. Bell, W. A., Daniel, B. R., and Zinn, B. T., "Experimental and Theoretical Determination of Admittances of a Family of Nozzles Subjected to Axial Instabilities," Journal of Sound and Vibration, Vol. 30, No. 2, pp. 179-190, September 1973.

13. Garrison, G. D., "Suppression of Combustion Oscillations with Mechanical Damping Devices," Interim Report PA FR-3299, Pratt and Whitney Aircraft Florida Research and Development Center, West Palm Beach, Florida, August 1969.

14. Lewis, G. D. and Garrison, G. D., "The Role of Acoustic Absorbers in Preventing Combustion Instability," AIAA/SAE 7th Propulsion Conferences, Salt Lake City, Utah, AIAA Paper No. 71-699, June 1971.

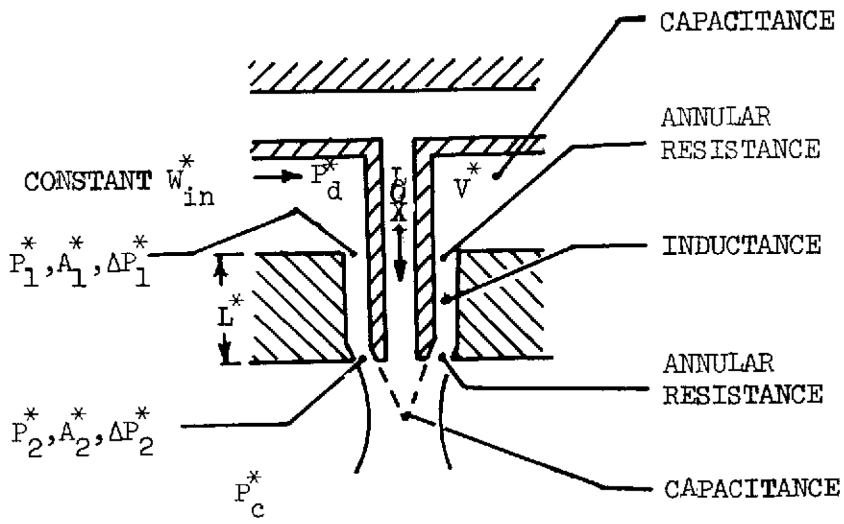

$$\frac{\bar{\rho}_d^* V^*}{\gamma \bar{W}^*} s\, P_d' = -W'$$

$$W' = \tfrac{1}{2}\left[\frac{\bar{P}_d^*}{\Delta P_1^*} P_d' + \left(\frac{1}{\gamma} - \frac{\bar{P}_1^*}{\Delta P_1^*}\right) P_1'\right]$$

$$P_1' - P_2' = \frac{\bar{W}^* L^*}{g \bar{P}_2^* A_1^*} sW'$$

$$W' = \tfrac{1}{2}\left[\frac{\bar{P}_2^*}{\Delta P_2^*} P_2' + \left(\frac{1}{\gamma} - \frac{\bar{P}_c^*}{\Delta P_2^*}\right) P_c'\right]$$

$$W_b' = W' e^{-\tau_b^* s}$$

Figure 1. Gaseous Hydrogen Injector.

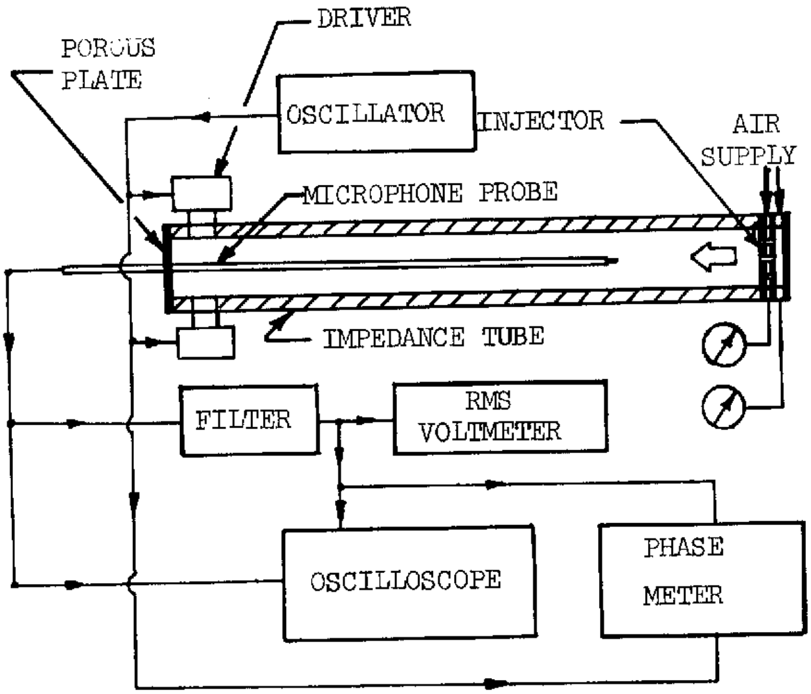

Figure 2. Experimental Apparatus

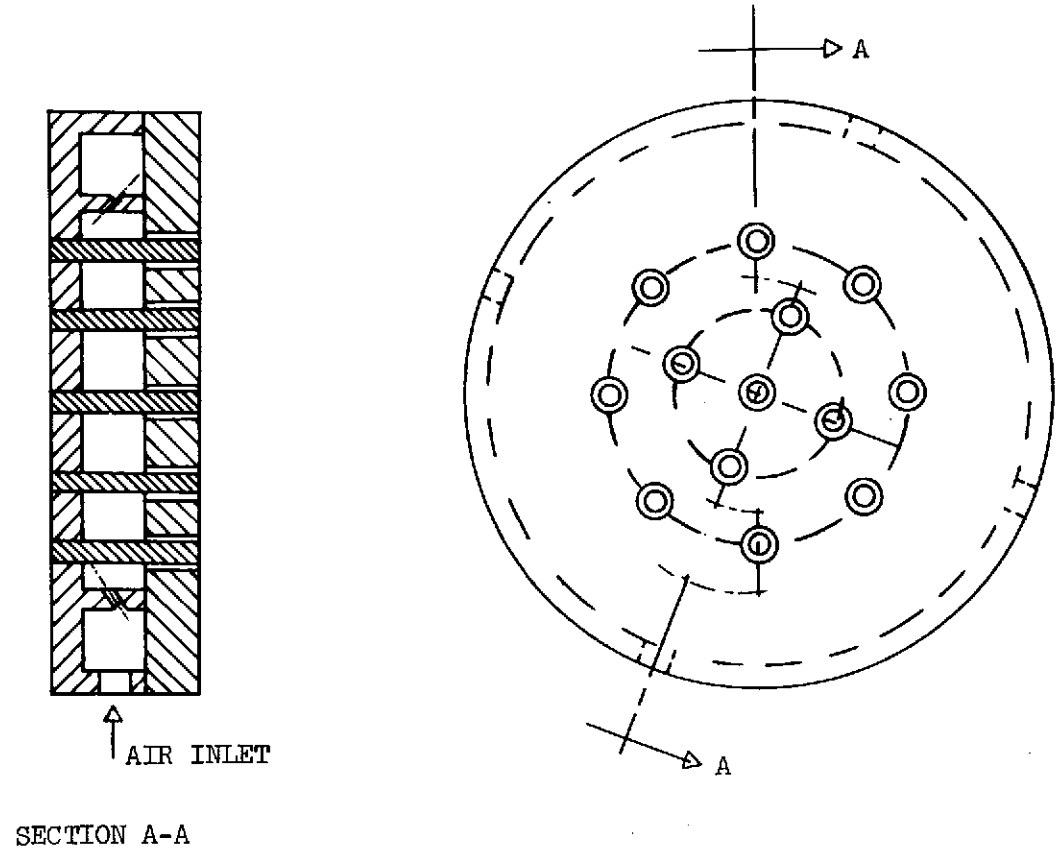

CONFIGURATION	σ(%)	L (IN.)	V (IN.^{3})
1	4.7	0.875	27.6

Figure 3. Description of Injector Configuration 1.

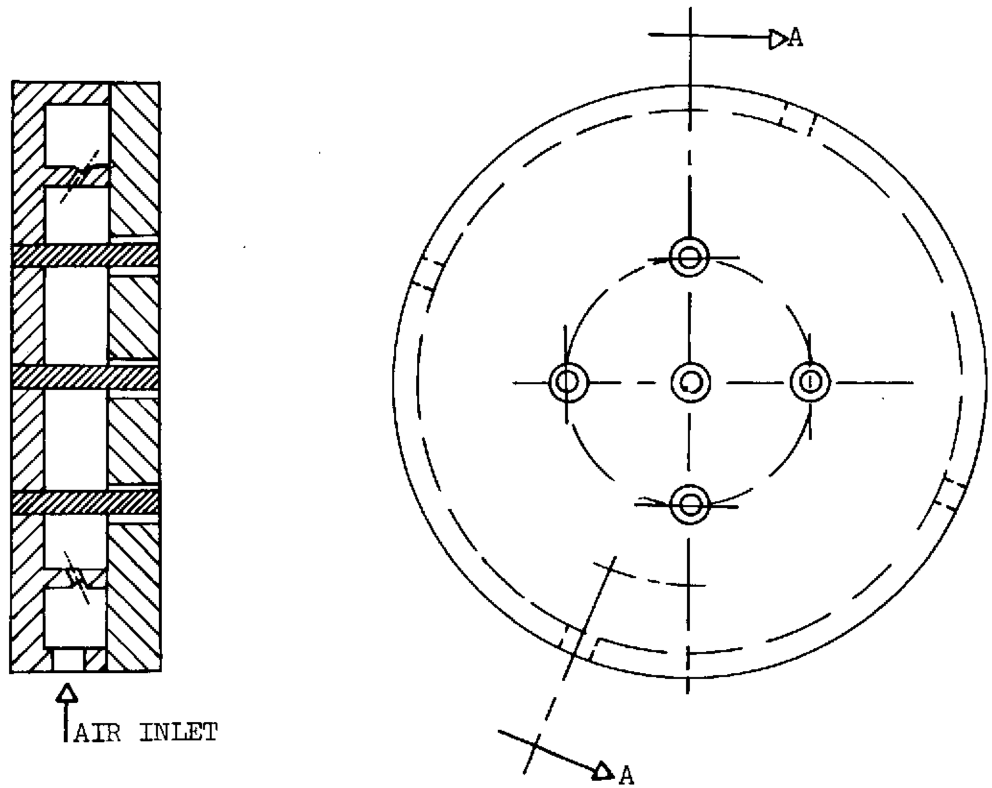

SECTION A-A

CONFIGURATION	σ (%)	L (IN.)	V (IN^3)
2	1.8	0.875	28.0

Figure 4. Description of Injector Configuration 2.

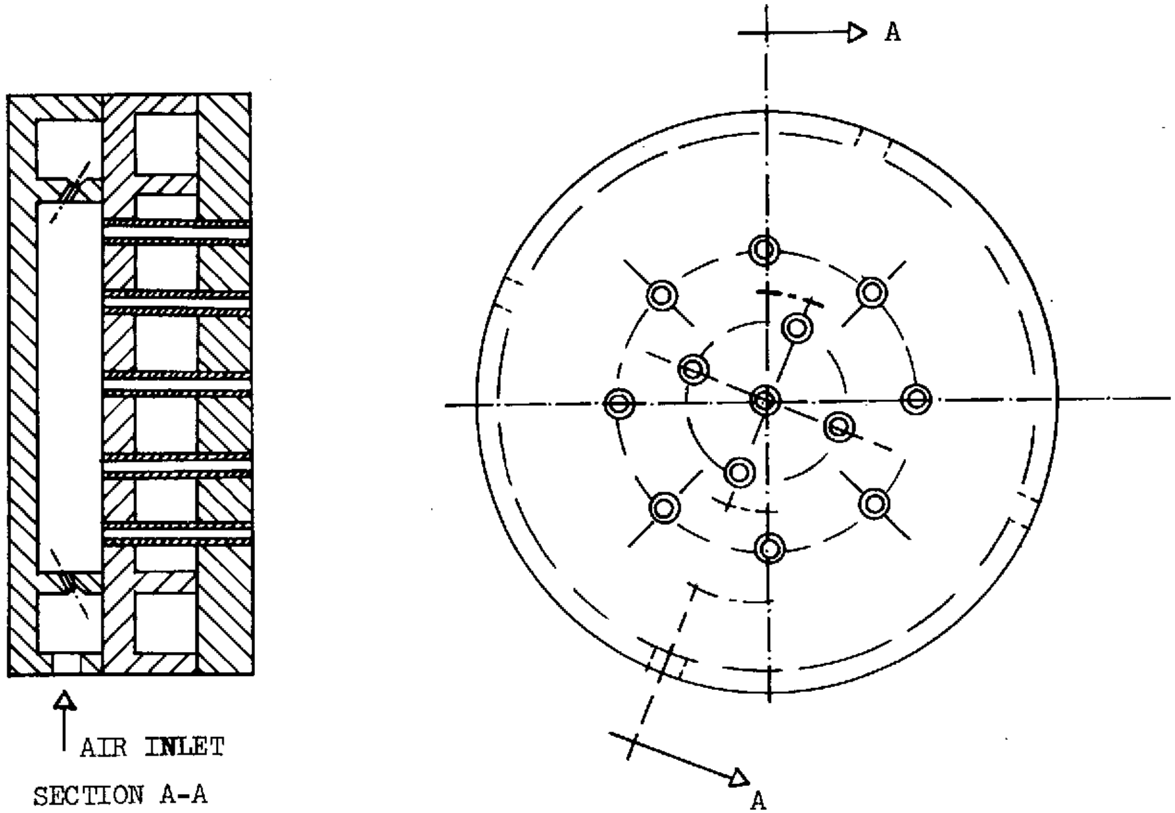

CONFIGURATION	σ (%)	L (IN.)	V(IN.^{3})
3	1.7	2.38	28.2
4	10.2	0.875	28.2
5	10.2	1.75	28.2

Figure 5. Descriptions of Injector Configurations 3, 4 and 5.

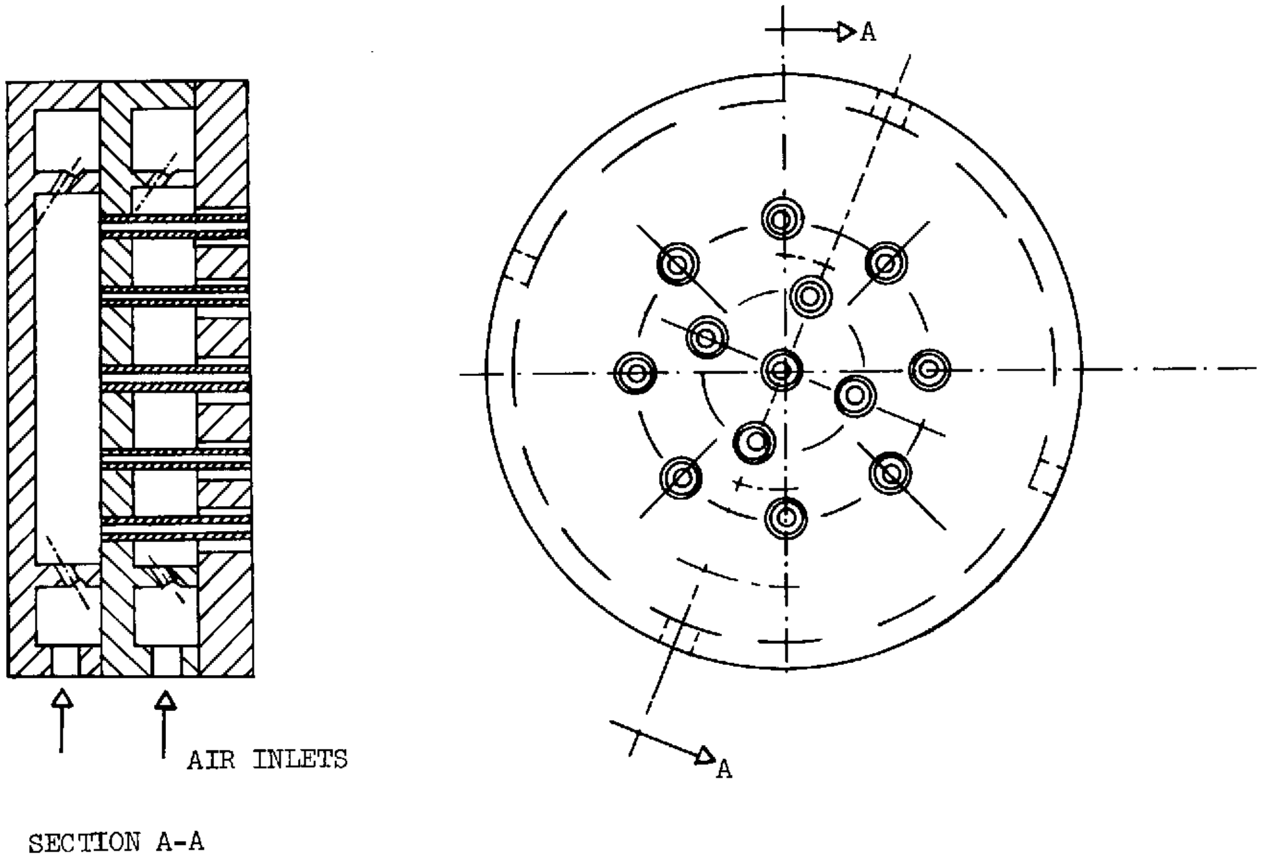

CONFIGURATION		σ (%)	L (IN.)	V(IN.^{3})
6	1	4.7	0.875	27.6
	3	1.7	2.38	28.2

Figure 6. Description of Injector Configuration 6.

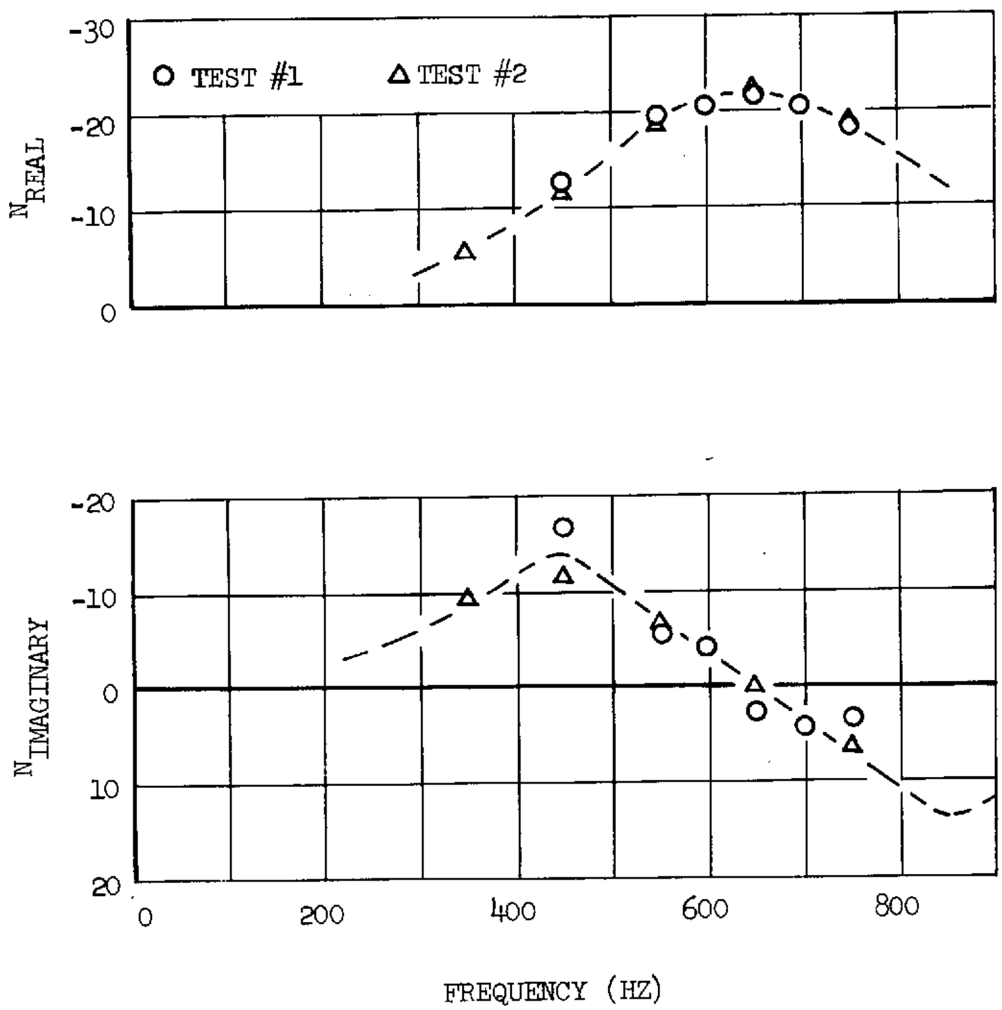

Figure 7. Repeatability of the Measured Response Factor Data.

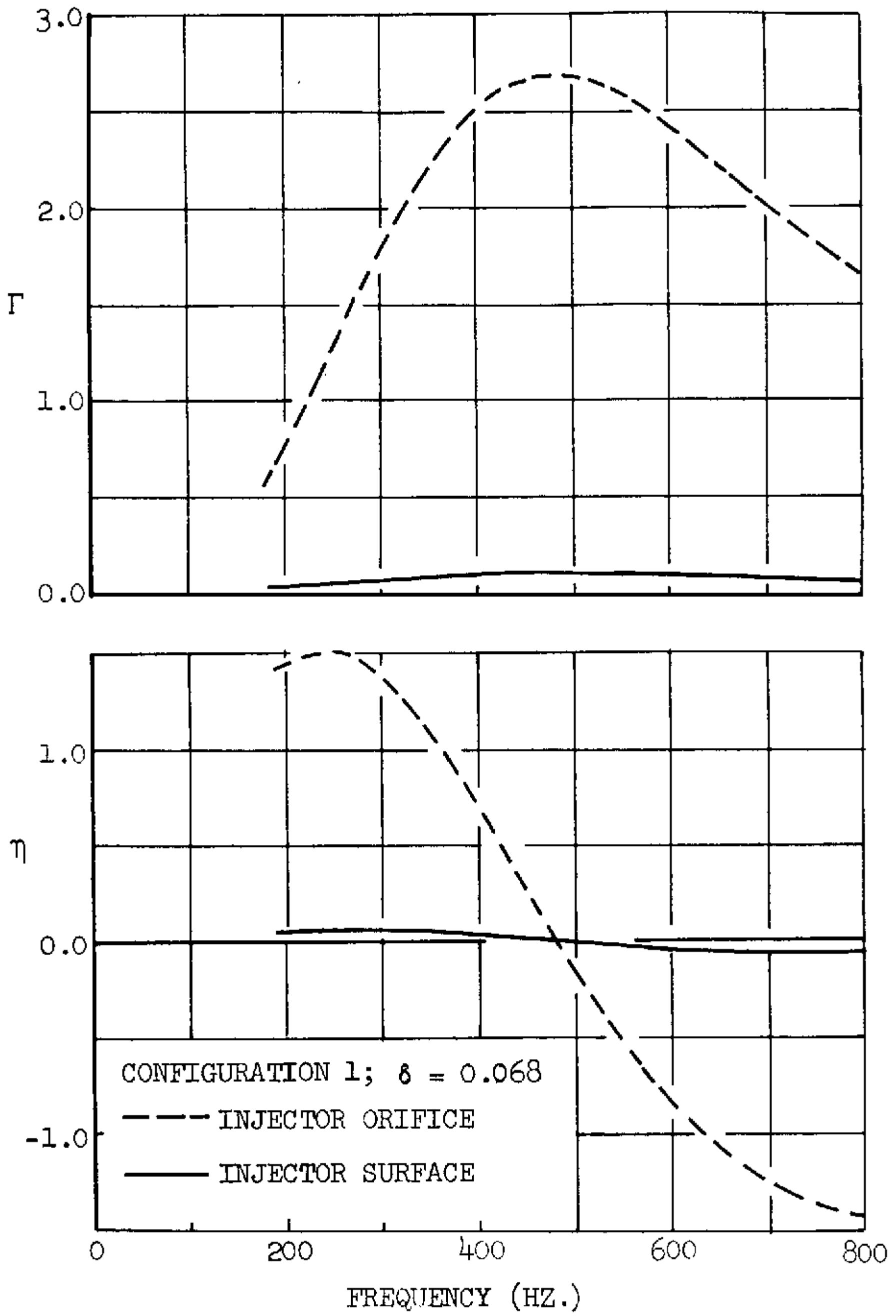

Figure 8. Predicted Admittances for the Injector Configuration 1.

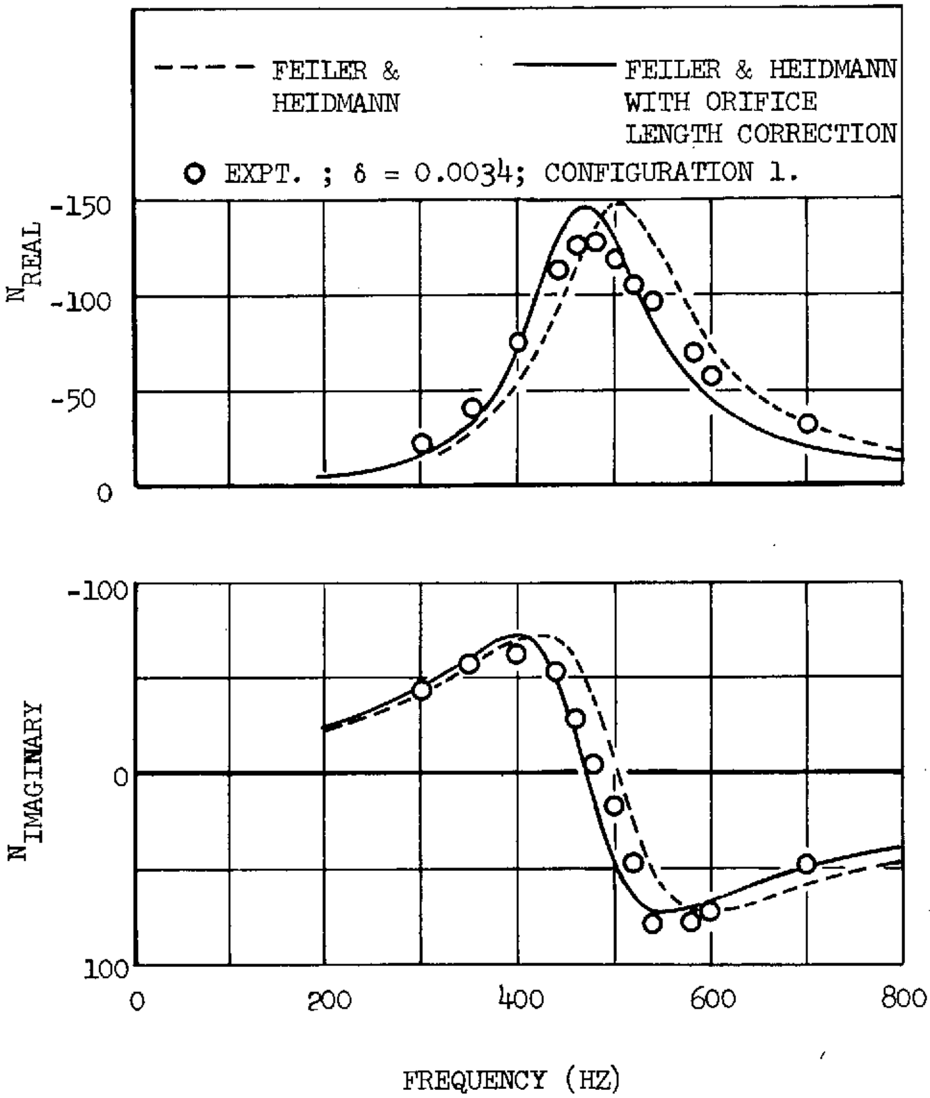

Figure 9. Feiler and Heidmann Predicted Response Factor Data with and without Orifice Length Correction.

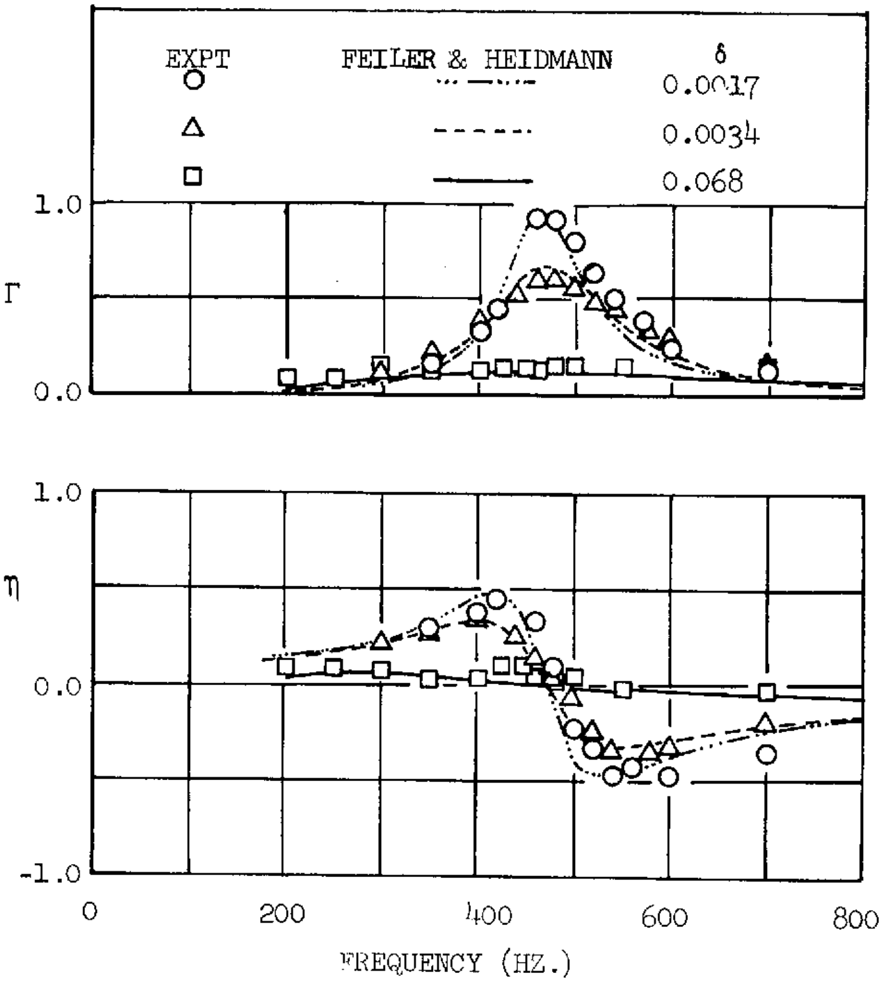

Figure 10. Frequency Dependence of the Surface Admittances of Injector Configuration 1.

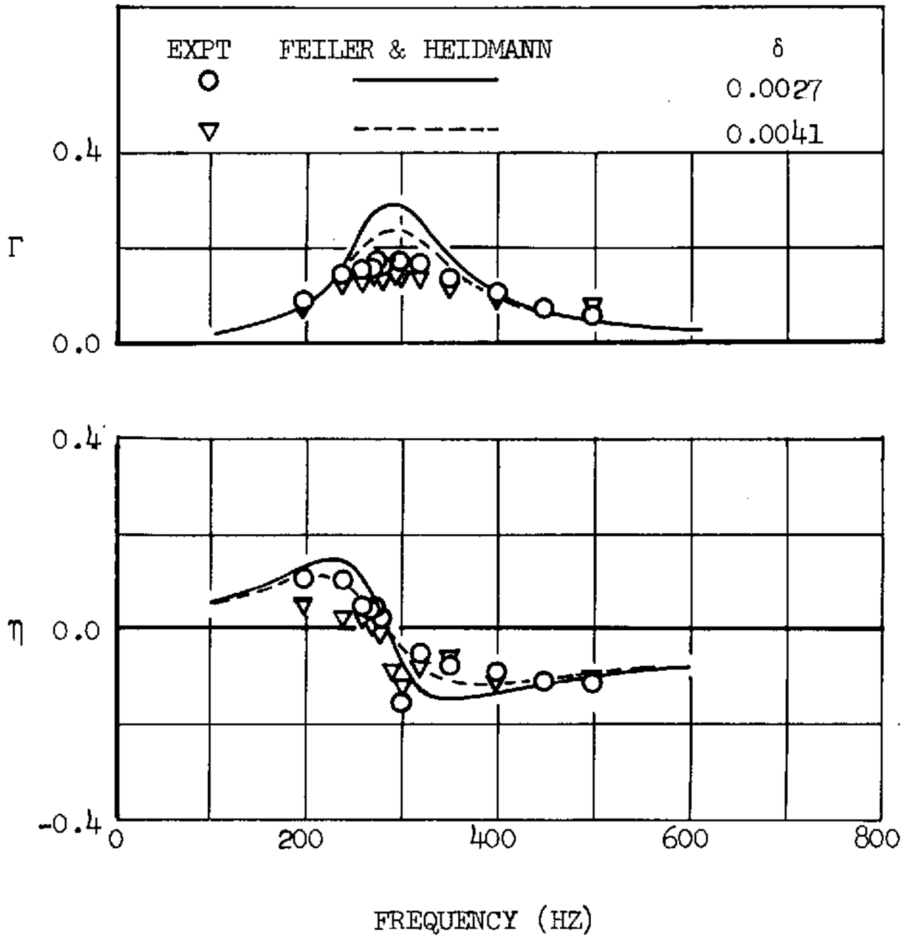

Figure 11. Frequency Dependence of the Surface Admittances of Injector Configuration 2.

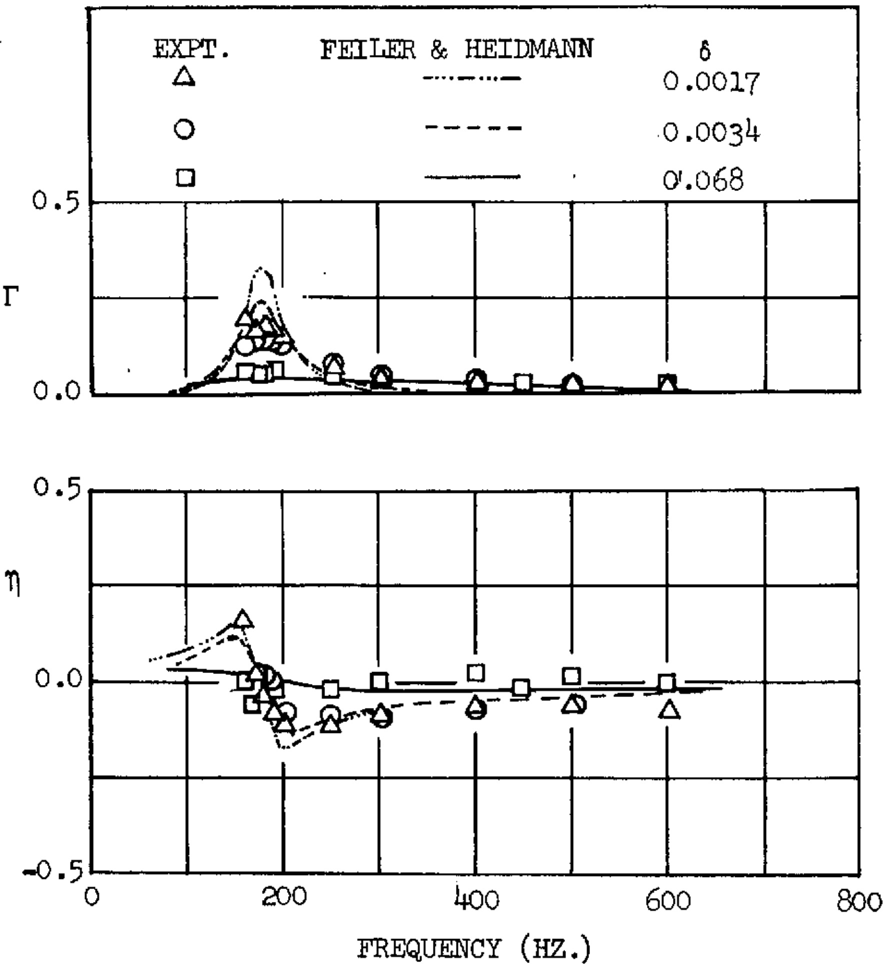

Figure 12. Frequency Dependence of the Surface Admittances of Injector Configuration 3.

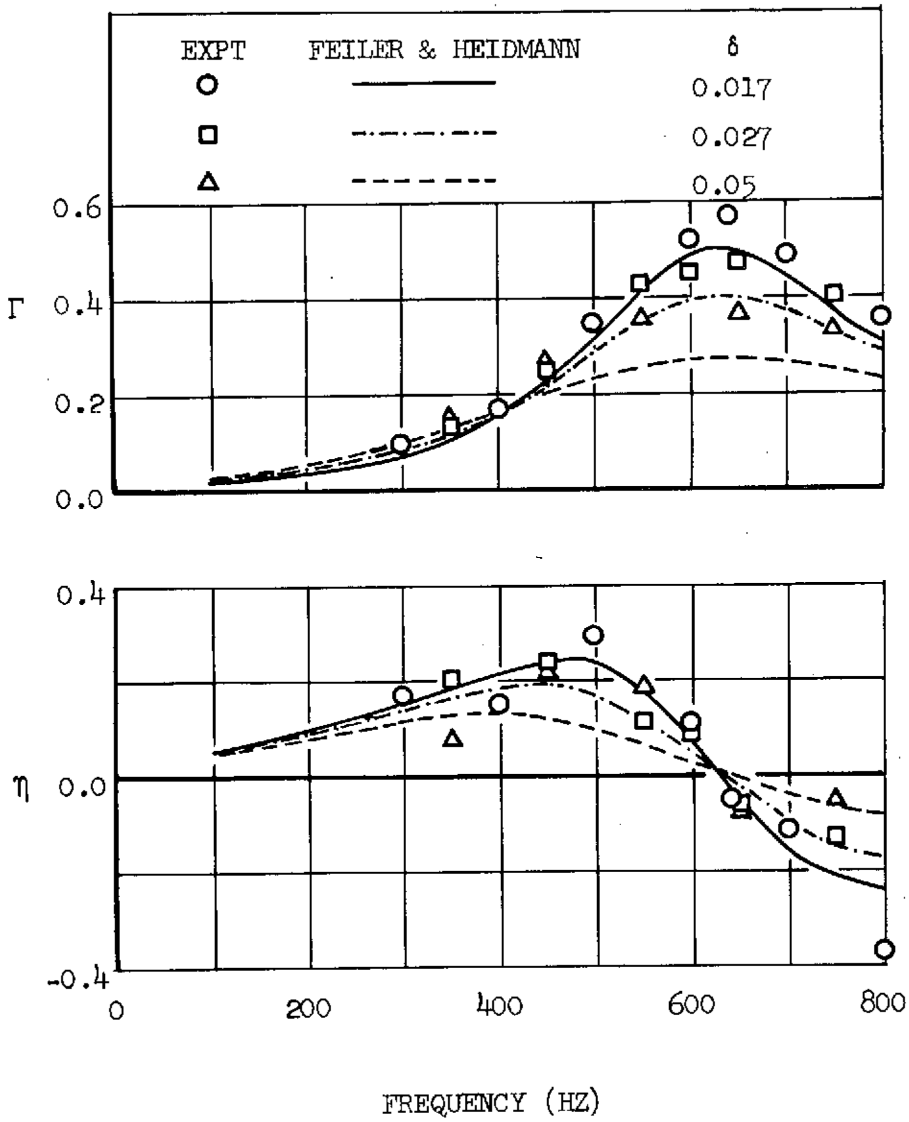

Figure 13. Frequency Dependence of the Surface Admittances of Injector Configuration 4.

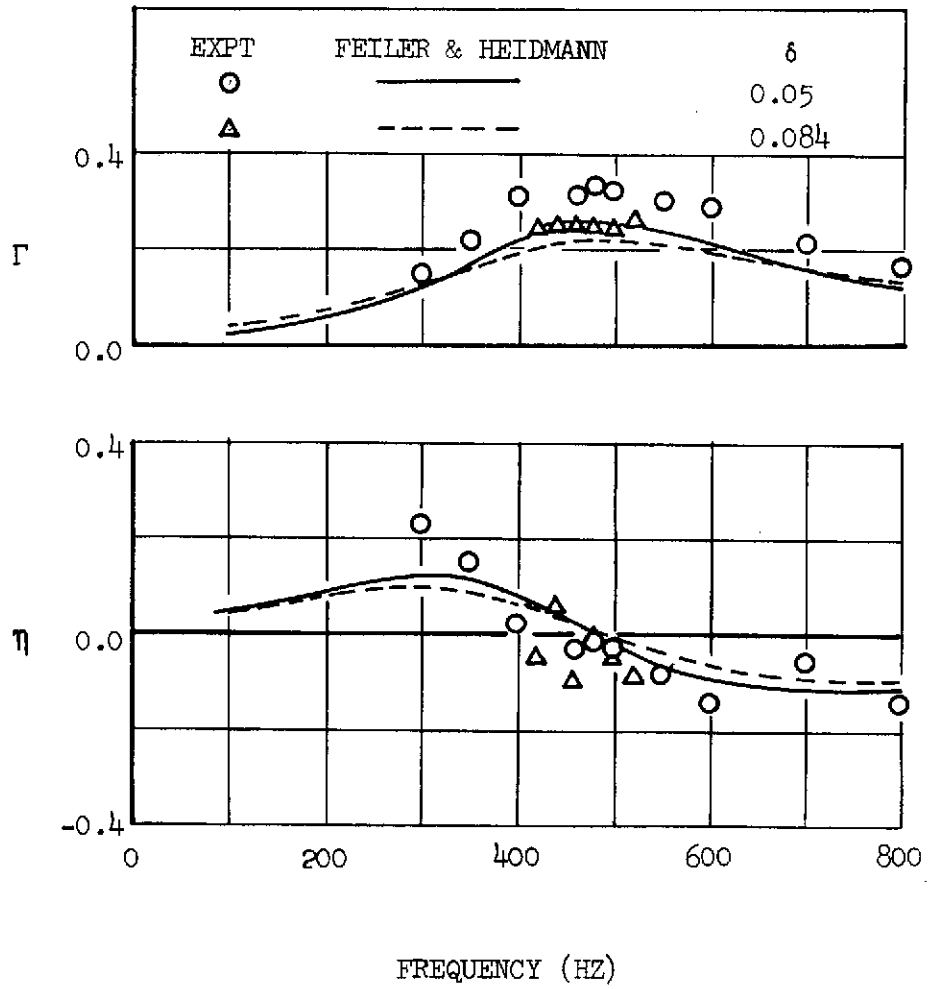

Figure 14. Frequency Dependence of the Surface Admittances of Injector Configuration 5.

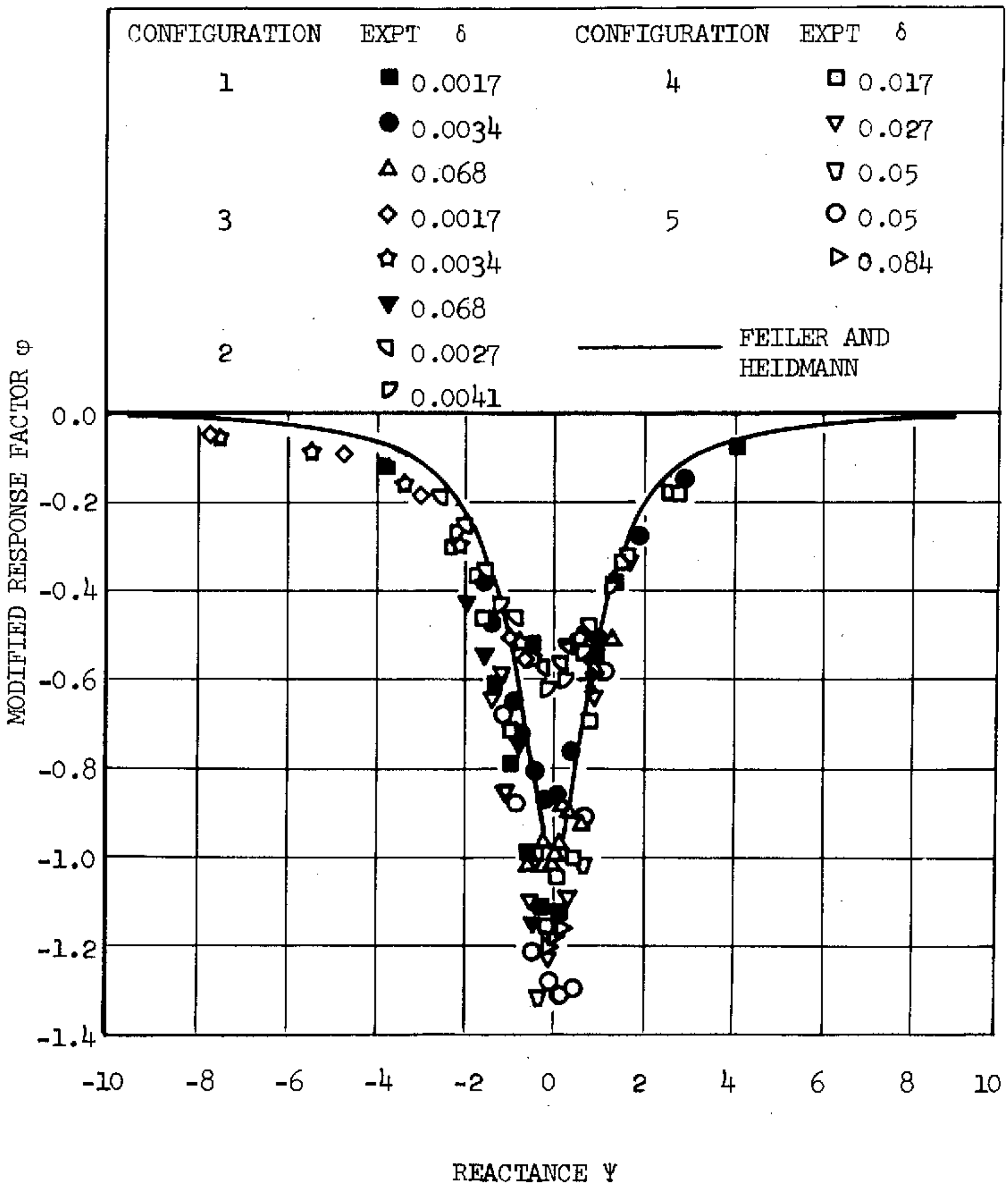

Figure 15. Generalized Response Factor Data Plotted Against Reactance.

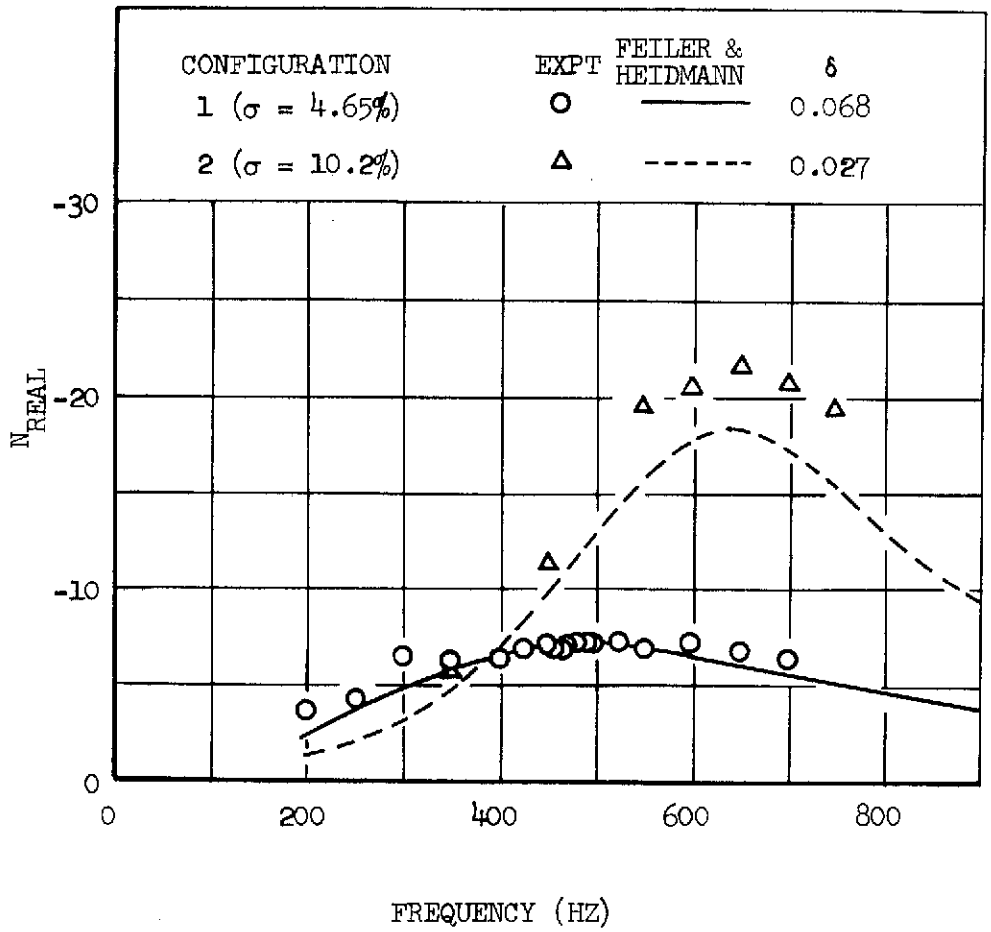

Figure 16. Effect of Open-Area Ratio on Injector Response Factor.

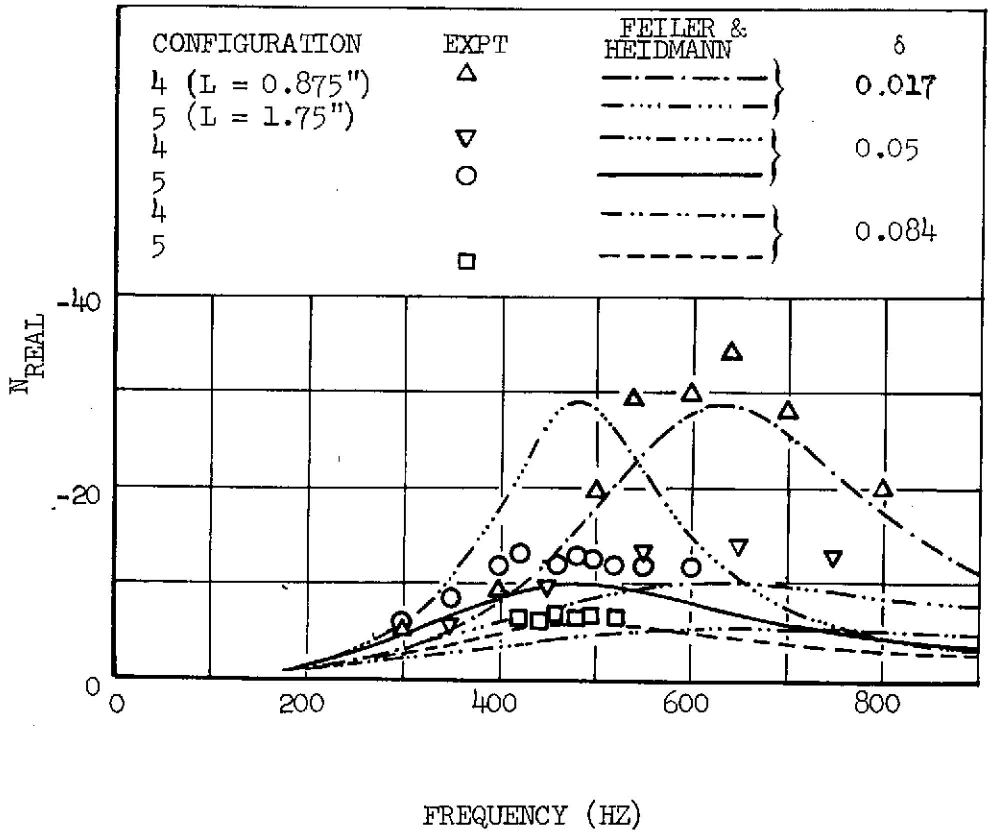

Figure 17. Effect of Orifice Length on Injector Response Factor.

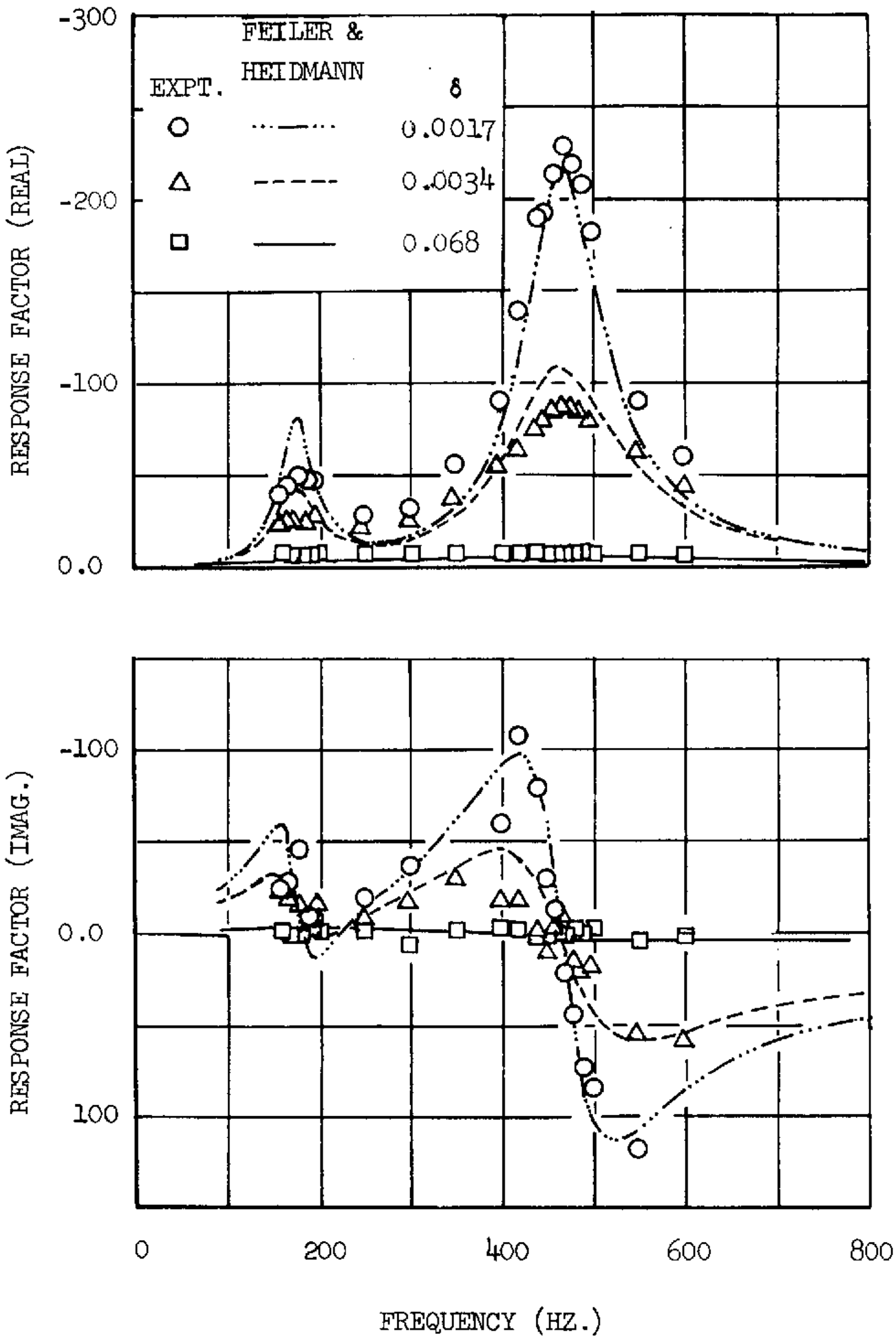

Figure 18. Frequency Dependence of Response Factors of Injector Configuration 6.

REPORT DISTRIBUTION LIST

NASA-Lewis Research Center
Attn: Dr. R. J. Priem/MS 500-204
21000 Brookpark Road
Cleveland, OH 44135
(2 copies)

NASA-Lewis Research Center
Attn: N. T. Musial/MS 500-311
21000 Brookpark Road
Cleveland, OH 44135

NASA-Lewis Research Center
Attn: Library/MS 60-3
21000 Brookpark Road
Cleveland, OH 44135

NASA-Lewis Research Center
Attn: Report Control Office/MS 5-5
21000 Brookpark Road
Cleveland, OH 44135

NASA-Lewis Research Center
Attn: E. A. Bourke/MS 500-205
21000 Brookpark Road
Cleveland, OH 44135

NASA Headquarters
Attn: RPS/Robert A. Wasel
600 Independence Ave., SW, Rm 526
Washington, DC 20546

NASA-Lewis Research Center
Attn: Procurement Section
Mail Stop 500-313
21000 Brookpark Road
Cleveland, OH 44135

NASA-Lyndon B. Johnson Space Center
Attn: EP/Joseph G. Thibodaux
Houston, TX 77058

NASA-George C. Marshall Space Flight Center
Attn: S&E-ASTN-PP/R. J. Richmond
Huntsville, AL 35812

Aerojet Liquid Rocket Company
Attn: David A. Fairchild
Bldg. 20001/Sec. 9732
P. O. Box 13222
Sacramento, CA 95813

Aerojet General Corporation
Propulsion Division
Attn: R. Stiff
P. O. Box 15847
Sacramento, CA 95803

Aerospace Corporation
Attn: O. W. Dykema
P. O. Box 92957
Los Angeles, CA 90045

Aerospace Corporation
Attn: Library-Documents
2400 E. El Segundo Boulevard
Los Angeles, CA 90045

Air Force Rocket Propulsion Lab. (RPM)
Attn. Library
Edwards, CA 93523

Air Force Office of Scientific Research
Chief Propulsion Division
Attn: Dr. J. F. Masi (NAE)
1400 Wilson Boulevard
Arlington, VA 22209

Air Force Rocket Propulsion Lab.
Attn: Daweel George
Edwards, CA 93523

AFAPL
Research & Technology Division
AF Systems Command
U. S. Air Force
Attn: Library/APRP
Wright Patterson AFB, OH 45433

NASA Scientific & Technical Information Facility - Acquisitions Br.
P. O. Box 33
College Park, MD 20740 (10 copies)

Army Ballistics Research Labs.
Attn: Austin W. Barrows
Code AMXBR-1B
Aberdeen Proving Grounds, MD 21005

Army Ballistic Research Labs.
Attn: Ingo W. May
Code AMXBR-1B
Aberdeen Proving Grounds, MD 21005

Army Material Command
Missile Systems Div.
Attn: Stephen R. Matos
Code AMCRD-MT
5001 Eisenhower Ave.
Alexandria, VA 22304

Air Force Systems Command
Arnold Engineering Development Center
Attn: Dr. H. K. Doetsch
Tullahoma, TN 37389

Aeronutronic Div. of Philco Ford Corporation
Technical Information Dept.
Ford Road
Newport Beach, CA 92663

Battelle Memorial Institute
Attn: Report Library, Room 6A
505 King Avenue
Columbus, OH 43201

Bell Aerosystems, Inc.
Attn: Library
Box 1
Buffalo, NY 14205

Bell Aerospace Company
Attn: T. F. Ferger
P. O. Box 1
Mail Zone, J-81
Buffalo, NY 14205

Air Force Rocket Propulsion Lab
Attn: Richard R. Weiss
Edwards, CA 93523

AFAPL
Attn: Frank D. Stull (RJT)
Wright Patterson AFB, OH 45433

California Institute of Technology
Jet Propulsion Laboratory
Attn: Fred E. C. Culick
4800 Oak Grove Drive
Pasadena, CA 91103

California Institute of Technology
Jet Propulsion Laboratory
Attn: Jack H. Rupe
4800 Oak Grove Drive
Pasadena, CA 91103

California State University
Sacramento School of Engineering
Attn: Frederick H. Reardon
6000 J. Street
Sacramento, CA 95819

Chemical Propulsion Information Agency
Johns Hopkins University/APL
Attn: T. W. Christian
8621 Georgia Avenue
Silver Spring, MD 20910

Colorado State University
Attn: Charles E. Mitchell
Fort Collins, CO 80521

Frankford Arsenal
Attn: Martin Visnov
NDP-R, Bldg. 64-2
Bridge & Tacony Streets
Philadelphia, PA 19137

General Electric Company
Flight Propulsion Lab. Dept.
Attn: D. Suichu
Cincinnati, OH 45215

Bureau of Naval Weapons
Department of the Navy
Attn: Library
Washington, DC

Brooklyn Polytechnic Institute
Long Island Graduate Center
Attn: V. D. Agosta
Route 110
Farmingdale, NY 11735

Marquardt Corporation
16555 Saticoy Street
Box 2013 - South Annex
Van Nuys, CA 91409

Massachusetts Institute of Tech.
Department of Mechanical Engr.
Attn: T. Y. Toong
77 Massachusetts Avenue
Cambridge, MA 02139

McDonald Douglas Corporation
McDonnell Douglas Astronautics Co.
Attn: William T. Webber
5301 Bolsa Ave.
Huntington Beach, CA 92647

D. E. Mock
Advanced Research Projects Agency
Washington, DC 20525

Lockheed Aircraft Corporation
Lockheed Propulsion Co., Div.
Attn: Norman S. Cohen
P. O. Box 111
Redlands, CA 92373

Naval Postgraduate School
Department of Aeronautics
Attn: David W. Netzer
Monterey, CA 93940

Naval Underwater Systems Center
Energy Conversion Dept.
Attn: Robert S. Lazar, Code 5B331
Newport, RI 02840

Georgia Institute of Technology
School of Aerospace Engineering
Attn: Warren C. Strahle
Atlanta, GA 30332

Georgia Institute of Technology
School of Aerospace Engineering
Attn: Ben T. Zinn
Atlanta, GA 30322

Melvin Gerstein
P. O. Box 452
Altadena, CA 91001

Ohio State University
Department of Aeronautical and
Astronautical Engineering
Attn: R. Edse
Columbus, OH 43210

Pennsylvania State University
Mechanical Engineering Dept.
Attn: G. M. Faeth
207 Mechanical Engineering Bldg.
University Park, PA 16802

Princeton University
Forrestal Campus Library
Attn: Irvin Glassman
P. O. Box 710
Princeton, NJ 08450

Princeton University
Forrestal Campus Library
Attn: David T. Harrje
P. O. Box 710
Princeton, NJ 08540

Princeton University
Forrestal Campus Library
Attn: Martin Summerfield
P. O. Box 710
Princeton, NJ 08540

Propulsion Sciences, Inc.
Attn: Vito Agosta
P. O. Box 814
Melville, NY 11746

Georgia Institute of Technology
School of Aerospace Engineering
Attn: Edward W. Price
Atlanta, GA 30332

Naval Weapons Center
Attn: Charles J. Thelan, Code 4305
China Lake, CA 93555

Naval Postgraduate School
Department of Aeronautics
Attn: Allen F. Fuhs
Monterey, CA 93940

Research and Development Associates
Attn: Raymond B. Edelman
P. O. Box 3580
525 Wilshire Blvd.
Santa Monica, CA 90402

Rockwell International Corp.
Rocketdyne Division
Attn: L. P. Combs, D/991-350
Zone 11
6633 Canoga Avenue
Canoga Park, CA 91304

Rockwell International Corp.
Rocketdyne Division
Attn: James A. Nestlerode
Dept. 596-124, AC46
6633 Canoga Ave.
Canoga Park, CA 91304

Rockwell International Corp.
Rocketdyne Division
Attn: Carl L. Oberg
Dept. 589-197-SS11
6633 Canoga Ave.
Canoga Park, CA 91304

Rockwell International Corp.
Rocketdyne Division
Attn: Library Dept. 596-306
6633 Canoga Avenue
Canoga Park, CA 91304

Purdue University
Jet Propulsion Laboratory
Project Squid
Attn: Robert Goulard
West Lafayette, IN 47907

Purdue University Res. Foundation
School of Mechanical Engineering
Attn: John R. Osborn
Thermal Sci. Propulsion Center
West Lafayette, IN 47906

Purdue University Res. Foundation
School of Mechanical Engineering
Attn: Bruce A. Reese
Thermal Sci. Propulsion Center
West Lafayette, IN 47906

Tennessee Technological University
Dept. of Mech. Engrg.
Attn: Kenneth R. Purdy
P. O. Box 5014
Cookeville, TN 38501

Textron, Inc.
Bell Aerospace, Div.
Research Department
Attn: John R. Morgenthaler, C-84
P. O. Box One
Buffalo, NY 14240

TRW, Inc.
TRW Systems Gp.
Attn: A. C. Ellings
One Space Park
Redondo Beach, CA 90278

TRW Systems
Attn: G. W. Elveran
One Space Park
Redondo Beach, CA 90278

TRW Systems Group
STL Tech. Lib. Doc. Acquisitions
One Space Park
Redondo Beach, CA 90278

Stanford Research Institute
333 Ravenswood Avenue
Menlo Park, CA 94025

Susquehanna Corporation
Atlantic Research Division
Attn: Library
Shirley Highway and Edsall Rd.
Alexandria, VA 22314

TISIA
Defense Documentation Center
Cameron Station, Bldg. 5
5010 Duke Street
Alexandria, Va. 22314

United Aircraft Corporation
Pratt & Whitney Aircraft Div.
Attn: Thomas C. Mayes
P. O. Box 2691
West Palm Beach, FL 33402

United Aircraft Corporation
United Technology Center
Attn: Library
P. O. Box 358
Sunnyvale, CA 94088

University of California, Berkeley
Dept. of Mechanical Engineering
Attn: A. K. Oppenheim
Berkeley, CA 94720

University of Michigan
Attn: James A. Nicholls
P. O. Box 622
Ann Arbor, MI 48107

University of Wisconsin
Mechanical Engineering Dept.
Attn: P. S. Myers
1513 University Avenue
Madison, WI 53706

Office of Assistnat Director
(Chemical Technician)
Office of the Director of Defense
Research & Engineering
Washington, DC 20301

Tulane University
Attn: J. C. O'Hara
6823 St. Charles Ave.
New Orleans, LA 70118

Ultrasystems, Inc.
Attn: Thomas J. Tyson
500 Newport Center Dr.
Newport Beach, CA

United Aircraft Corp.
Pratt & Whitney Division
Florida Research & Development
Center
Attn: Library
West Palm Beach, FL 33402

United Aircraft Corporation
Attn: R. H. Woodward Waesche
400 Main Street
East Hartford, CT 06108

University of California
Aerospace Engineering Dept.
Attn: F. A. Williams
P. O. Box 109
LaJolla, CA 92037

University of Illinois
Aeronautics/Astronautic Eng. Dept.
Attn: R. A. Strehlow
Trans. Bldg., Room 101
Urbana, IL 61801

University of Utah
Dept. of Chemical Engineering
Attn: Alva D. Baer
Bark Bldg., Room 307
Salt Lake City, UT 84112

U. S. Naval Research Laboratory
Director (Code 6180)
Attn: Library
Washington, DC 20390

Virginia Polytechnic Institute
State University
Attn: J. A. Schetz
Blacksburg, VA 24061